Proc. Natl. Acad. Sci. USA
Vol. 87, pp. 8805–8809, November 1990
Biochemistry

X-ray crystallographic structure of a complex between a synthetic protease of human immunodeficiency virus 1 and a substrate-based hydroxyethylamine inhibitor

(AIDS/retrovirus/diastereomer/tetrahedral intermediate/symmetry)

AMY L. SWAIN*†, MARIA M. MILLER*, JEREMY GREEN‡, DANIEL H. RICH‡, JENS SCHNEIDER§, STEPHEN B. H. KENT§¶, AND ALEXANDER WLODAWER*

*Crystallography Laboratory, National Cancer Institute-Frederick Cancer Research and Development Center, ABL-Basic Research Program, Frederick, MD 21702; ‡School of Pharmacy and Department of Chemistry, University of Wisconsin-Madison, Madison, WI 53706; §Division of Biology, California Institute of Technology, Pasadena, CA 91125; and ¶Graduate School of Science and Technology, Bond University, Gold Coast, Queensland, Australia 4229

Communicated by Bruce Merrifield, August 2, 1990

ABSTRACT **The structure of a crystal complex of the chemically synthesized protease of human immunodeficiency virus 1 with a heptapeptide-derived inhibitor bound in the active site has been determined. The sequence of the inhibitor JG-365 is Ac-Ser-Leu-Asn-Phe-ψ[CH(OH)CH_2N]-Pro-Ile-Val-OMe; the K_i is 0.24 nM. The hydroxyethylamine moiety, in place of the normal scissile bond of the substrate, is believed to mimic a tetrahedral reaction intermediate. The structure of the complex has been refined to an *R* factor of 0.146 at 2.4-Å resolution by using restrained least squares with rms deviations in bond lengths of 0.02 Å and bond angles of 4°. The bound inhibitor diastereomer has the *S* configuration at the hydroxyethylamine chiral carbon, and the hydroxyl group is positioned between the active site aspartate carboxyl groups within hydrogen bonding distance. Comparison of this structure with a reduced peptide bond inhibitor–protease complex indicates that these contacts confer the exceptional binding strength of JG-365.**

Reverse transcriptase, integrase, and protease are the three virally encoded enzymes necessary for replication of human immunodeficiency virus 1 (HIV-1), so each is a potential target for drug design. Rational design of drugs directed against AIDS would be greatly facilitated by knowledge of the three-dimensional structures of the target molecules, yet the protease is the only one of these enzymes for which the structure of the native form (1–3) or of an inhibitor complex (4) is known. The protease is a member of the well-characterized family of aspartic proteases, which also includes mammalian enzymes such as renin, pepsin, and chymosin. Whereas cell-encoded aspartic proteases are monomers with distinct amino and carboxyl domains, the retroviral proteases are dimers of identical subunits that are analogous to these domains (5). The function of the HIV-1 protease is to cleave the translated viral gag–pol polyprotein into discrete components. Without protease activity, the viral particle remains noninfective (6, 7) and this property makes the protease an attractive candidate for therapeutic drug design against AIDS (8–14).

Inhibitors of aspartic proteases have been developed as potential pharmaceutical agents for modulating the biological processes catalyzed by this class of enzymes (15, 16). Most efforts in recent years have been directed toward developing antihypertensive drugs that inhibit the aspartic protease renin (17) and the principles that were discovered have greatly facilitated the design of inhibitors of HIV-1 protease. The best inhibitors are derived from substrate sequences by replacing the dipeptide cleavage site with stable analogs of reaction pathway intermediates (18–22). Extremely potent inhibitors of HIV-1 protease contain a hydroxyethylamine (HEA) linkage, which is believed to mimic a tetrahedral intermediate of substrate hydrolysis (14, 22). These compounds have been shown to effectively inhibit processing of a synthetic substrate (14, 22) and of the HIV-1 gag–pol polyprotein (14) *in vitro*. It has also been demonstrated directly that several of the protease inhibitors have antiviral activity in tissue cultures (12–14).

Herein we report the structure‖ of a synthetic HIV-1 protease complexed with an HEA inhibitor, JG-365, and compare it with a complex structure in which the reduced peptide bond inhibitor MVT-101 was 3000 times less potent (4). The results substantiate a previously proposed mechanism of action for this class of enzymes (23) and have implications for the design of other inhibitors of HIV-1 protease. Inhibitor JG-365, which has the sequence Ac-Ser-Leu-Asn-Phe-ψ[CH(OH)CH_2N]-Pro-Ile-Val-OMe, was used as a mixture of both the *R* and *S* diastereomers. The mixture has a K_i of 0.66 nM against synthetic HIV-1 protease, whereas the pure *S* diastereomer has a K_i of 0.24 nM (C. Q. Sun and M. V. Toth, personal communication). MVT-101, the reduced peptide bond inhibitor with the sequence Ac-Thr-Ile-Nle-ψ(CH_2NH)-Nle-Gln-Arg (where Nle is norleucine), is used as a reference and has a K_i of 780 nM.

MATERIALS AND METHODS

HIV-1 [$Aba^{67,95}$]protease (where Aba is L-α-amino-*n*-butyric acid) was chemically synthesized as previously described (24, 25). The sequence used was that of the SF2 isolate with cysteines replaced by L-α-amino-*n*-butyric acid (2). The inhibitor JG-365 was synthesized as described (22). The K_i values were measured at pH 6.5 (22).

Crystals were grown by vapor diffusion using the hanging-drop technique. Conditions in the reservoir were 55–60% (vol/vol) saturated ammonium sulfate/≈0.1 M sodium acetate, pH 5.4. The protein concentration was ≈5 mg/ml. The inhibitor was dissolved in dimethyl sulfoxide and diluted into the protein sample to give a final inhibitor concentration of 9 mg/ml [9% (vol/vol) dimethyl sulfoxide]. The 6-μl drops consisted of 50% of this mixture and 50% of the protein–inhibitor sample. Crystals grew at ≈23°C in 3 days.

The publication costs of this article were defrayed in part by page charge payment. This article must therefore be hereby marked "*advertisement*" in accordance with 18 U.S.C. §1734 solely to indicate this fact.

Abbreviations: HIV-1, human immunodeficiency virus 1; HEA, hydroxyethylamine.

†To whom reprint requests should be addressed.

‖The atomic coordinates have been deposited in the Protein Data Bank, Chemistry Department, Brookhaven National Laboratory, Upton, NY 11973 (reference 7HVP).

The crystal used for data collection measured 0.06 × 0.1 × 0.4 mm and was mounted in a quartz capillary. Data were collected using a Siemens area detector mounted on a three-axis camera. The data extended to 2.4 Å and were complete to 2.5 Å [5398 reflections with $I > 1.5\ \sigma(I)$ from 10 to 2.4 Å were included in refinement]. The merging R factor on I was 8.9%.

The protease–JG-365 complex crystallized in space group $P2_12_12_1$ in a crystal form isomorphous to that of the protease–MVT-101 complex (4). The unit-cell parameters were a = 51.2 Å, b = 58.8 Å, c = 62.0 Å, $\alpha = \beta = \gamma = 90°$, with a homodimeric protein molecule and one inhibitor molecule in the asymmetric unit. An initial difference electron density map was generated by using phases calculated from atomic coordinates of the protein alone from the structure of the protease–MVT-101 complex. A model of JG-365 was built to fit this density and the structure of the complex was refined using the restrained least squares program PROFFT (26, 27) to an R factor of 0.262. After 12 cycles of refinement the R factor was lowered to 0.246 with an overall B of 12.0 Å^2. Electron density maps were calculated with the coefficients $(2|F_o| - |F_c|)\alpha_c$ and $(|F_o| - |F_c|)\alpha_c$ (where F_o is the observed structure factor, F_c is the calculated structure factor, and α_c is the calculated phase). Refinement continued and solvent was included with manual rebuilding interventions.

RESULTS

The final model includes 1516 protein atoms, 61 inhibitor atoms, and 95 solvent atoms with the geometrical parameters listed in Table 1. The R factor calculated at the completion of refinement is 0.146, with a mean temperature factor for all protein atoms of 15.1 Å^2. Monomer 1 is numbered from 1 to 99, monomer 2 is numbered from 101 to 199, and JG-365 is numbered from 201 to 207. The first water listed in the coordinates, water-301 [water-511 in the protease–MVT-101 complex (4)], is particularly important for binding the inhibitor. A comparison of this complex and the protease–MVT-101 complex shows 34 solvent molecules common to both structures, occupying positions within 1 Å.

The conformation of the protease in the complex with JG-365 can be considered the same as in the protease–MVT-101 complex and is more compact than the native enzyme, where the flaps are distant from the active site. The rms deviation between α carbons of the protein in the two complexes is 0.37 Å; for all atoms the difference is 0.43 Å for 1363 pairs of atoms.

Table 1. Summary of the geometrical parameters for the structure of the HIV-1 protease–JG-365 complex

	Target σ	rms δ (observed)
Distances, Å		
Bonded distances	0.02	0.02
Angle distances	0.04	0.06
Planar 1–4 distances	0.05	0.05
Planar groups, Å	0.02	0.02
Chiral volume, Å^3	0.15	0.21
Nonbonded distances, Å		
Single torsion	0.30	0.22
Multiple torsion	0.30	0.26
Possible hydrogen bonds	0.30	0.26
Thermal restraints, Å^2		
Main chain bond	1.5	1.2
Main chain angle	2.0	1.9
Side chain bond	3.0	3.5
Side chain angle	4.0	4.8
Torsion angles, deg		
Planar	3	2.4
Staggered	10	21.9
Orthonormal	20	14.8

Target σ values (weights) used in PROFFT are given as well as the rms deviations from ideality.

In the protease–JG-365 complex, the inhibitor is positioned in a single orientation in the protease active site with the flaps folded directly over it, protecting the inhibitor from bulk solvent. The position and orientation of the inhibitor were obvious from the first difference electron density map calculated, and the electron density was further improved during refinement (Fig. 1). The HEA hydroxyl group is nestled between the side-chain carboxyl groups of the two active site aspartates within hydrogen bonding distance. The bonding is asymmetric with Asp-25 slightly closer than Asp-125. This asymmetry and the distances are comparable to what was found in other aspartyl protease–inhibitor complexes (23).

To verify the orientation of the inhibitor, residue-deleted maps were used to fit it in the reverse direction. The reversed inhibitor model, after refinement, did not fit well to its own $(2|F_o| - |F_c|)\alpha_c$ map, and the $(|F_o| - |F_c|)\ \alpha_c$ map showed negative peaks where there were atoms and positive peaks where there were not. Since the original inhibitor fit this map quite well, our data give no evidence of inhibitor disorder in this complex.

Although the inhibitor contained approximately equal amounts of R and S configurations at the HEA chiral carbon (22), only the tighter-binding S diastereomer was observed in the enzyme–inhibitor complex. To verify these results, we built a model of the R diastereomer, maintaining all other contacts between the inhibitor and protein. After restraining this configuration in several cycles of least squares refinement, difference electron density maps displayed a peak of negative density in the position of the hydroxyl group of the R diastereomer and a positive peak in the region where the hydrogen atom would be (the position of the hydroxyl group in the S diastereomer). This confirmed that only the S diastereomer was observed in the enzyme–inhibitor complex.

In addition to the contact between the hydroxyl group on the tetrahedral carbon and the active site aspartates, polar contact between inhibitor and enzyme was made through only one substituent atom of the Asn-203 side chain (P_2) (Fig. 2); it is

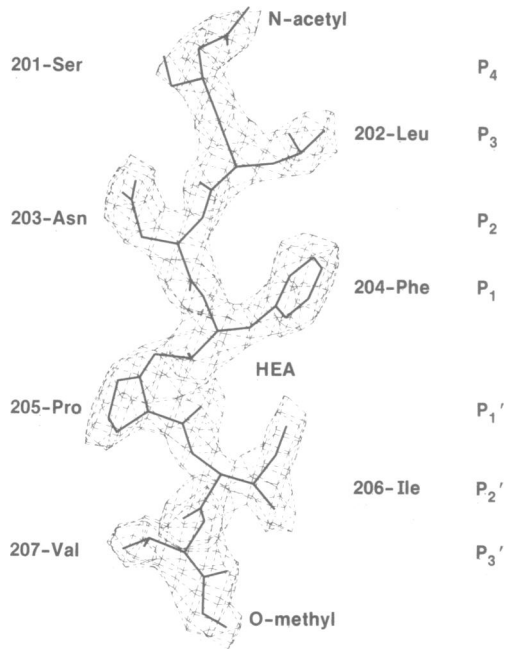

FIG. 1. Model of the inhibitor JG-365 superimposed on the $(2|F_o| - |F_c|)\alpha_c$ electron density contoured at the 1-σ level. The residues are labeled (P_4–P_3') from the amino to carboxyl terminus, with the HEA linkage at the P_1–P_1' junction.

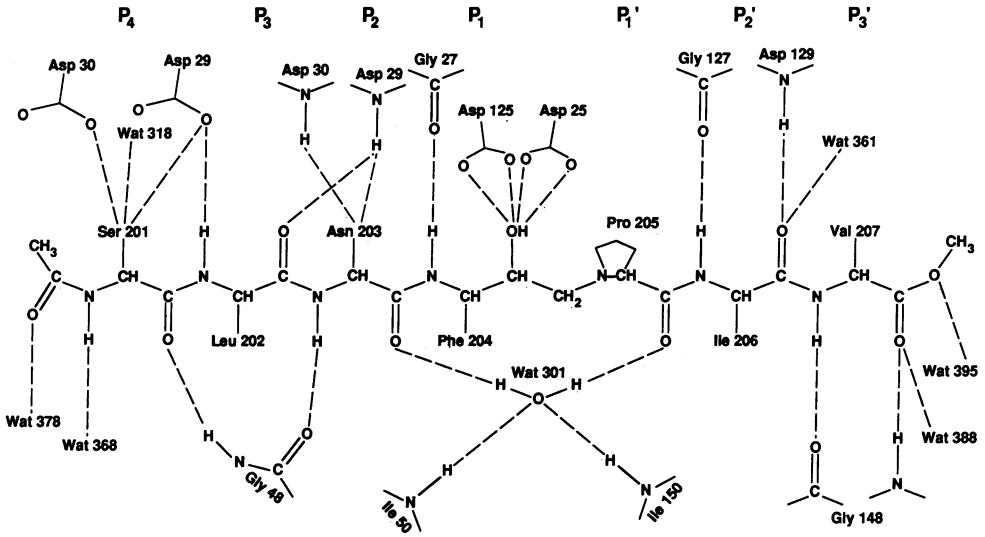

FIG. 2. Schematic representation of the hydrogen bond interactions among the inhibitor JG-365, the protein, and the solvent. Wat, water.

currently modeled as oxygen. There was no density present for the Ser-201 (P_4) hydroxyl group so it was positioned to optimize contacts. The oxygens of the N-terminal acetyl group and the C-terminal methoxy group hydrogen bond with water molecules (Fig. 2) and the carbonyl oxygen of the methoxy group makes contact with the nitrogen of Gly-148 (a similar contact was made through only a water molecule in the protease–MVT-101 complex). The C-terminal amide nitrogen of P_3' in MVT-101 is not present in JG-365 so the contact between the inhibitor and side chain of Asp-129 is lost.

The anchoring hydrogen bonds between the JG-365 inhibitor backbone atoms and the protein are similar to those reported for the protease–MVT-101 structure (4), although JG-365 is one amino acid longer on the N-terminal end. Torsion angles for the backbone of JG-365 are listed in Table 2. Fig. 3 shows the superposition of JG-365 and MVT-101. The rms difference in α-carbon positions of the two inhibitors is 0.56 Å; for main-chain atoms the difference is 0.78 Å. The major difference in the main chains is seen at the P_1–P_1' linkage site. There are only subtle differences between hydrophobic contacts of the protease–JG-365 complex and those of the protease–MVT-101 complex (4).

Water-301, located between the flaps and the inhibitor (Fig. 2), plays a critically important role in the interactions between the enzyme and inhibitors bound at the active site. Water-301 was also observed in the protease–MVT-101 complex (water-511). Its role appears to be important in inducing the fit of the flaps over the inhibitor. The carbonyls of inhibitor residues 203 and 205 are hydrogen bond acceptors of water-301 and two main-chain nitrogen atoms from the flaps are hydrogen bond donors, resulting in tetrahedral coordination of the water. This water molecule may help to maintain asymmetry in the protein molecule as it mediates the contact between the tips of the flaps and the inhibitor.

Table 2. Torsion angles for JG-365

Residue	Backbone dihedral angles, deg		
	ϕ	ψ	ω
201	−64	169	180
202	−123	138	−178
203	−143	104	180
204	−94	47	151, −12
205	−57	174	175
206	−130	122	−177
207	−143	138	

Backbone dihedral angles for JG-365 in the enzyme–inhibitor complex are listed. With the exception of the HEA linkage (residues 204–205), these angles correspond to an extended conformation of peptide.

Although the HIV-1 protease dimer in the enzyme–inhibitor complex is composed of identical polypeptide chains, the perfect twofold symmetry present in the unliganded enzyme (2) is lost. Deviations from ideal twofold symmetry may arise in part because the inhibitor is inherently asymmetric. Large differences are observed at the interdimer interface that are believed to be caused by intermolecular crystal contacts between the asymmetric protein dimers. Fig. 4 shows the positional differences in the α carbons of the two monomers.

The regions of notable deviations between the two monomers appear to be directly related to inhibitor binding. One of these regions is the loop 49–52 (Fig. 5); the difference between the α carbons upon superposition of Gly-49 and

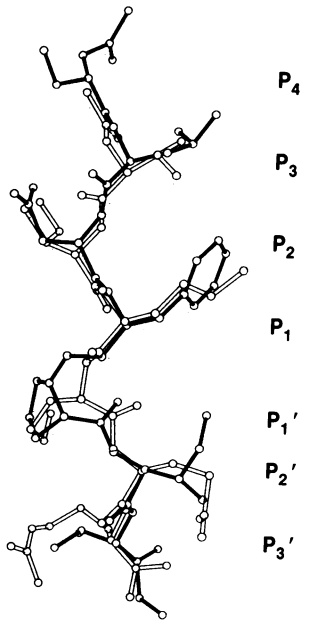

FIG. 3. Superposition of the heptapeptide inhibitor JG-365 and the hexapeptide reduced-peptide bond inhibitor MVT-101. The RIGID option in FRODO (28) was used to superimpose the P_3–P_3' α-carbon atoms of these inhibitors. Only JG-365 has a residue (serine) at position P_4.

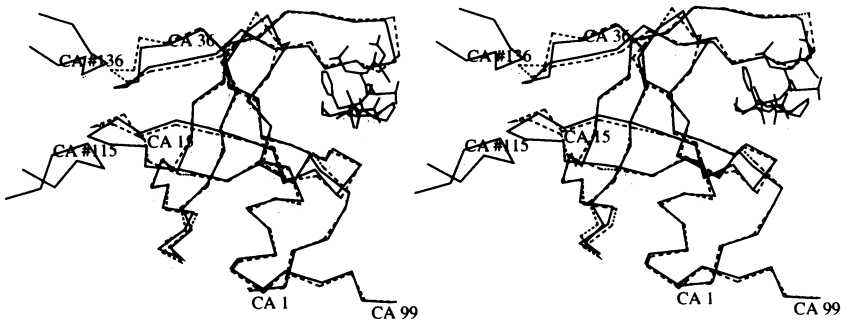

FIG. 4. Superposition of the α carbons of monomer 2 (dashed line) on monomer 1 (solid line) relative to the all-atom model of JG-365. The amino and carboxyl termini of the protein are labeled (1 and 99) and the regions of significant differences are identified with a reference label on a residue within that region. The short segments (solid line) to the left of the protease are those regions of a symmetry-related molecule that affect the positions of the loops through crystal-packing interactions. These are identified by a symbol (#) by the reference point. It should be noted that the symmetry-related subunit adjacent to monomer 1 is monomer 2.

Gly-149 is 1.6 Å. These loop regions are the tips of the flaps that close over the inhibitor and provide some side-chain contacts to the hydrophobic binding pockets. It has been pointed out (4) that these flaps rearrange themselves with respect to the native protease and close over the inhibitor such that the two flaps have very similar positions. The positions are not equivalent because the peptide bond between residues Ile-50 and Gly-51 is turned 180° compared with that between Ile-150 and Gly-151. This provides a means for a direct hydrogen bond between the tips of the flaps. Fig. 5 depicts the resulting positional differences in the loose loop regions of residues 79–81 and 179–181. This region appears to be different from one monomer to the other because the flap peptide bond orientations are different. Loop 79–81 is in contact with loop 149–152 through water-312. Loop 149–152 is then in a direct stabilizing contact with loop 49–52. Loop 49–52 hydrogen bonds to water-342 and makes no contacts with loop 179–181, because its conformation is and must be different from loop 149–152 to fit tightly over the inhibitor. It may be significant that there are crystal lattice contacts between the side chains of the flaps and side chains of the adjacent symmetry-related molecule. However, it cannot be proven whether the observed changes addressed above are due to inhibitor binding or to crystal lattice contacts.

The largest differences in α-carbon positions between monomer 1 and monomer 2 are along the β loop of residues 15–18 and the loose loop 37–40 (Fig. 4); these differences are probably due to crystal packing. Each of these loops packs against its own symmetry mate, mutually but not identically affecting the conformation of the residues in the loops. The temperature factors in these regions are the highest in the whole protein structure, with loop 15–18 having higher temperature factors in monomer 2 but loop 37–40 having higher temperature factors in monomer 1.

DISCUSSION

Analysis of the structure of the complex between HIV-1 protease and JG-365, in comparison with the weaker-binding inhibitor MVT-101 (4), provides some rationale for the tight binding associated with JG-365. The major difference between the two inhibitors is the interaction of the hydroxyl group in JG-365 with the catalytically active Asp-25 and Asp-125 carboxyl groups. This hydroxyl group is known to be critically important to binding since JG-365 binds to protease $>10^3$- to -10^4-fold tighter than closely related inhibitors that lack the hydroxyl group (9). The remaining hydrogen bonds for both inhibitors, especially those involving the backbone amide bonds, are very similar.

The HEA dipeptidyl unit differs from a true isosteric analog of a reaction intermediate in substrate hydrolysis by the presence of one extra backbone atom contained in the methylene adjacent to the CH(OH) group. The added methylene group must be accommodated by the enzyme, and this structure reveals that the added methylene requires the inhibitor to adopt a conformation of P_1' not directly analogous to that of MVT-101. The inhibitor backbone is kinked so that the P_1' proline ring is pushed deep into the S_1' binding pocket (Fig. 3). In this regard, the proline residue is acting more as a hydrophobic side chain than as a normal peptide unit. However, this binding mode must be quite favorable. It is also evident from the electron density maps that the proline ring not contained in a true amide bond is distorted relative to a normal puckered conformation for proline.

It is particularly interesting that only the *S* diastereomer of JG-365 is seen in the crystal structure. This is consistent with the finding that the *S* analogs of JG-365 are much more potent inhibitors of protease than the corresponding *R* diastereomers (D.H.R. and C. Q. Sun, unpublished results). These results contrast with those of Roberts *et al.* (14) who found a 2-fold preference for binding of the *R* diastereomer of moderate HEA inhibitors that span the P_3–P_2' residues; however, a large difference in K_i was observed between the diastereomers of an optimized inhibitor: the *R* diastereomer of the Phe-PIC (where PIC is piperidine-(2*S*)-carbonyl) HEA analogue was 235-fold more potent than the *S* diastereomer.

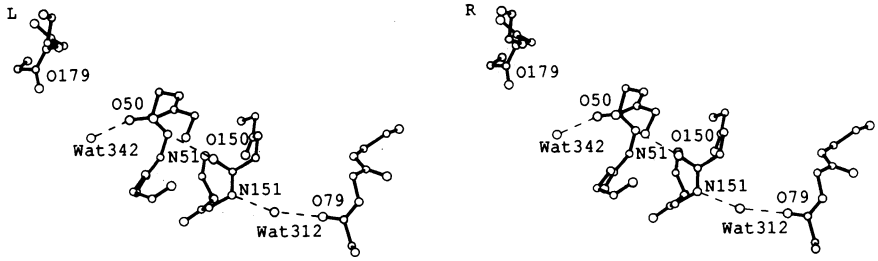

FIG. 5. Stereo view of only those regions of the protease that are apparently directly affected by binding of JG-365. The dashed lines represent hydrogen bonds. The relevant backbone atoms and water molecules involved are labeled. The distance between 0-179 and 0-342 is 4.3 Å. Wat, water.

These inhibitors lack a P_3' substituent, whereas it is the incorporation of P_3' into JG-365 that leads to a 600-fold increase in its binding to the protease (22). Furthermore, in the protease–JG-365 and protease–MVT-101 complexes, the P_3' side chain of the inhibitor forms the outer wall of the S_1' hydrophobic binding pocket. The absence of the P_3' moiety could account for the weakened binding of JG-365 analogs that lack the P_3' functionality; it might also allow alternative tight-binding modes for inhibitors with the *R* configuration in the HEA linkage.

We can use the structure of the protease–JG-365 complex to examine possible contributions to the catalytic mechanism for this aspartic protease and to see if this offers insight for the design of protease inhibitors. If we assume that the HEA group mimics a reaction pathway intermediate, we can superimpose the gem diol group of a tetrahedral intermediate over the CH(OH) group in the HEA unit and place the proline nitrogen in the position of the methylene carbon in the HEA unit, where it would be found in the substrate. In this position, the proline nitrogen, which approaches tetrahedral geometry as the adjacent carbonyl group loses trigonal planar character, lies about 3.1 Å from the outer Δ oxygen of Asp-25. Our model is consistent with the features of the aspartic protease general acid–general base catalytic mechanism proposed by Suguna *et al.* (23). This means that the hydroxyl group on the tetrahedral carbon of JG-365 represents the position of the nucleophile, assuming that attack came from that water in the active site of the native enzyme that was seen in the structure of protease from Rous sarcoma virus (29).

The major difference between the structures of complexes of HIV-1 protease and inhibitors and those of cell-encoded aspartic proteases and inhibitors (23, 30) lies in the role of water-301. This water molecule, which is present in both HIV-1 protease–inhibitor complexes, serves to mediate hydrogen bonds between the two flaps and the inhibitors. If water-301 exists in the protease–substrate complexes as well, it would establish hydrogen bonds between the enzyme flaps and the substrate. The resulting hydrogen bonds would exert strain on the scissile amide bond, causing it to rotate out of plane and lose double-bond character. These interactions would significantly enhance the vulnerability of the P_1–P_1' bond toward hydrolysis, providing a means for the strain (31) necessary for the proposed mechanism (23). Because the Pro-205 nitrogen of the substrate would be within hydrogen bonding distance of the outer Δ oxygen of Asp-25, this would further stabilize the strained intermediate. The presence of water-301 suggests that it should be possible to develop selective inhibitors for retroviral proteases that require this structural feature, which would lead to more selective therapeutic agents.

We thank Annaliese Palmer for providing computed coordinate sets for JG-365. The Advanced Scientific Computing Laboratory (Frederick Cancer Research and Development Center) provided a substantial allocation of time on their CRAY X-MP supercomputer. Research sponsored in part by the National Cancer Institute (Department of Health and Human Services) Contract NO1-CO-74101 with ABL, by funds from the National Science Foundation Biological Instrumentation Division to S.B.H.K., and by National Institutes of Health Grant AI27302 to D.H.R.

1. Navia, M. A., Fitzgerald, P. M. D., McKeever, B. M., Leu, C.-T., Heimback, J. C., Herber, W. K., Sigal, I. S., Darke, P. L. & Springer, J. P. (1989) *Nature (London)* **337**, 615–620.
2. Wlodawer, A., Miller, M., Jaskólski, M., Sathyanarayana, B. K., Baldwin, E., Weber, I. T., Selk, L. M., Clawson, L., Schneider, J. & Kent, S. B. H. (1989) *Science* **245**, 616–621.
3. Lapatto, R., Blundell, T., Hemmings, A., Overington, J., Wilderspin, A., Wood, S., Merson, J. R., Whittle, P. J., Danley, D. E., Geoghegan, K. F., Hawrylik, S. J., Lee, S. E., Scheld, K. G. & Hobart, P. M. (1989) *Nature (London)* **342**, 299–302.
4. Miller, M., Schneider, J., Sathyanarayana, B. K., Toth, M. V., Marshall, G. R., Clawson, L., Selk, L., Kent, S. B. H. & Wlodawer, A. (1989) *Science* **246**, 1149–1152.
5. Pearl, L. H. & Taylor, W. R. (1987) *Nature (London)* **329**, 351–354.
6. Seelmeier, S., Schmidt, H., Turk, V. & von der Helm, K. (1988) *Proc. Natl. Acad. Sci. USA* **85**, 6612–6616.
7. Mous, J., Heimer, E. P. & Le Grice, S. F. J. (1988) *J. Virol.* **62**, 1433–1436.
8. Moore, M. L., Bryan, W. M., Fakhoury, S. A., Magaard, V. W., Huffman, W. F., Dayton, B. D., Meek, T. D., Hyland, L., Dreyer, G. B., Metcalf, B. W., Strickler, J. E., Gorniak, J. G. & Debouck, C. (1989) *Biochem. Biophys. Res. Commun.* **159**, 420–425.
9. Dreyer, G. B., Metcalf, B. W., Tomaszek, T. A., Jr., Carr, T. J., Chandler, A. C., III, Hyland, L., Fakhoury, S. A., Magaard, V. W., Moore, M. L., Strickler, J. E., Debouck, C. & Meek, T. D. (1989) *Proc. Natl. Acad. Sci. USA* **86**, 9752–9756.
10. Sigal, I. S., Huff, J. R., Darke, P. L., Vacca, J. P., Young, S. D., Desolms, J. S., Thompson, W. J., Lyle, T. A., Graham, S. L. & Ghosh, A. K. (1989) Eur. Patent Appl. 0,337,714.
11. Billich, S., Knoop, M.-T., Hansen, J., Strop, P., Sedlacek, J., Mertz, R. & Moelling, K. (1988) *J. Biol. Chem.* **263**, 17905–17908.
12. Meek, T. D., Lambert, D. M., Dreyer, G. B., Carr, T. J., Tomaszek, T. A., Jr., Moore, M. L., Strickler, J. E., Debouck, C., Hyland, L. J., Matthews, T. J., Metcalf, B. W. & Petteway, S. R. (1990) *Nature (London)* **343**, 90–92.
13. McQuade, T. J., Tomasselli, A. G., Liu, L., Karacostas, V., Moss, B., Sawyer, T. K., Heinrickson, R. L. & Tarpley, W. G. (1990) *Science* **247**, 454–456.
14. Roberts, N. A., Martin, J. A., Kinchington, D., Broadhurst, A. V., Craig, J. C., Duncan, I. B., Galpin, S. A., Handa, B. K., Kay, J., Kröhn, A., Lambert, R. W., Merrett, J. H., Mills, J. S., Parkes, K. E. B., Redshaw, S., Ritchie, A. J., Taylor, D. L., Thomas, G. J. & Machin, P. J. (1990) *Science* **248**, 358–361.
15. Rich, D. H. (1988) in *Research Monographs in Cell and Tissue Physiology*, eds. Barrett, A. J. & Salvesen, G. (Elsevier, Amsterdam), Vol. 12, pp. 179–217.
16. Rich, D. H. (1990) in *Comprehensive Medicinal Chemistry*, ed. Sammes, P. G. (Pergamon, Oxford), Vol. 2, pp. 391–441.
17. Greenlee, W. (1987) *Pharm. Res.* **4**, 364–374.
18. Szelke, M., Leckie, B., Hallett, A., Jones, D. M., Sueiras, J., Atrash, B. & Lever, A. F. (1982) *Nature (London)* **299**, 555–557.
19. Szelke, M., Jones, D. M., Atrash, B. & Hallett, A. (1983) *Pept. Struct. Funct. Proc. Am. Symp. 8th*, 579–583.
20. Dann, J. G., Stammers, D. K., Harris, C. J., Arrowsmith, R. J., Davies, D. E., Hardy, G. W. & Morton, J. A. (1986) *Biochem. Biophys. Res. Commun.* **134**, 71–77.
21. Ryono, D. E., Free, C. A., Neubeck, R., Samaniego, S. G., Godfrey, J. D. & Petrillo, E. W. (1985) *Pept. Struct. Funct. Proc. Am. Pept. Symp. 9th*, 739–742.
22. Rich, D. H., Green, J., Toth, M. V., Marshall, G. R. & Kent, S. B. H. (1990) *J. Med. Chem.* **33**, 1285–1288.
23. Suguna, K., Padlan, E. A., Smith, C. W., Carlson, W. D. & Davies, D. R. (1987) *Proc. Natl. Acad. Sci. USA* **84**, 7009–7013.
24. Kent, S. B. H. (1988) *Annu. Rev. Biochem.* **57**, 957–989.
25. Schneider, J. & Kent, S. B. H. (1988) *Cell* **54**, 363–368.
26. Hendrickson, W. A. (1985) *Methods Enzymol.* **115**, 252–270.
27. Finzel, B. C. (1987) *J. Appl. Crystallogr.* **20**, 53–55.
28. Jones, T. A. (1978) *J. Appl. Crystallogr.* **11**, 268–272.
29. Miller, M., Jaskólski, M., Rao, J. K. M., Leis, J. & Wlodawer, A. (1989) *Nature (London)* **337**, 576–579.
30. Blundell, T. L., Cooper, J., Foundling, S. I., Jones, D. M., Atrash, B. & Szelke, M. (1987) *Biochemistry* **26**, 5585–5590.
31. Jencks, W. P. (1969) in *Catalysis in Chemistry and Enzymology* (McGraw-Hill, New York), pp. 294–308.